ACS APPLIED MATERIALS & INTERFACES

www.acsami.org

Research Article

Three Polyhedron-Based Metal−Organic Frameworks Exhibiting Excellent Acetylene Selective Adsorption

Xia Zhou, Zitong Song, Rajamani Krishna, Lixiaoxiao Shi, Kangli Zhang, and Dongmei Wang*

Cite This: *ACS Appl. Mater. Interfaces* 2024, 16, 41542−41550

Read Online

ACCESS | Metrics & More | Article Recommendations | Supporting Information

ABSTRACT: The separation of acetylene (C_2H_2) from ethylene (C_2H_4) and ethane (C_2H_6) is crucial for the production of high-purity C_2H_2 and the recovery of other gases. Polyhedron-based metal−organic frameworks (PMOFs) are characterized by their spacious cavities, which facilitate gas trapping, and cage windows with varying sizes that enable gas screening. In this study, we carefully selected a class of PMOFs based on V-type tetracarboxylic acid linker (**JLU-Liu22** containing benzene ring, **JLU-Liu46** containing urea group and recombinant reconstructed **In/Cu CBDA** on the basis of **JLU-Liu46**) to study the relationship between pore environment and C_2 adsorption and separation performance. Among the three compounds, **JLU-Liu46** exhibits superior selectivity toward C_2H_2/C_2H_4 (2.06) as well as C_2H_2/C_2H_6 (2.43). Comparative structural analysis reveals that the exceptional adsorbed-C_2H_2 performance of **JLU-Liu46** can be attributed to the synergistic effects arising from coordinatively unsaturated Cu sites combined with an optimal pore environment (matched pore size and polarity, urea functional group), resulting in a strong affinity between the framework and C_2H_2 molecules. Furthermore, transient breakthrough simulations of **JLU-Liu46** confirmed its potential for separating C_2H_2 in ternary C_2 gas.

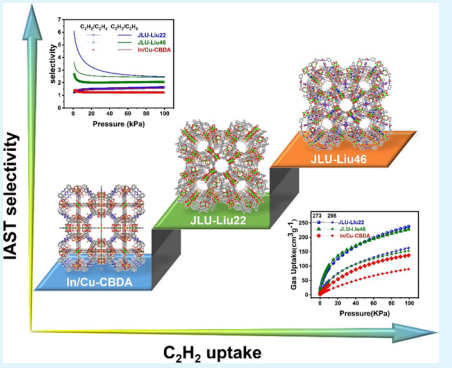

KEYWORDS: *metal−organic frameworks, polyhedron-based cage, pore engineering, C_2H_2 storage, gas adsorption and separation*

INTRODUCTION

High-purity acetylene (C_2H_2) is a basic raw material for the production of various chemicals and polymers, such as acrylic acid, butylene glycol, polyvinyl chloride, acrylic acid derivatives, etc.[1−3] However, it is principally produced by steam cracking of hydrocarbons or the partial combustion methane methods and is inevitably mixed with ethylene (C_2H_4) or ethane (C_2H_6).[4−6] Based on the structure of the carbon−carbon bonds, their molecular sizes, boiling points, and electronegativity/shape are very similar[7−9] (Table S1). Therefore, the separation of C_2H_2 from $C_2H_6/C_2H_4/C_2H_2$ mixtures is a crucial and challenging task.[10] Current technology for recovering C_2H_2 from other gases generally relies on cryogenic distillation or solvent extraction, which results in high energy consumption and negative environmental impact.[11,12] In recent years, adsorptive separation technology based on porous materials has been considered a promising feasibility method, which has the advantages of energy saving, environmental benefits, and high efficiency.[13]

Polyhedron-based metal−organic frameworks (PMOFs) have a large-void cage interconnected through windows of different sizes and open channels, which gives them the opportunity to construct PMOFs with large pore volumes, high surface areas, and excellent selective gas absorption capacities.[14,15] Notably, the typical PMOF materials composed of V-type tetracarboxylate linkers and $[Cu_2(COO)_4]$ paddlewheel units have an extraordinary specific surface area.[16−19] The C≡C triple bond within the molecular structure of C_2H_2 forms a strong interaction with the open metal sites (OMSs) in the PMOFs. Therefore, functionalized O/N sites[20] and OMSs are introduced to enhance the adsorption capacity of C_2H_2 gas, thereby improving separation efficiency. For example, based on the V-type tetracarboxylic acid ligand, Liu et al. reported PMOF JLU-Liu21[21] with high-density LBS/OMSs by introducing functional groups rich in N/O sites, which made it have outstanding gas adsorption capacity. For the PCN-306[22] material studied by Chen and co-workers, the experiments found that V-type carboxylic ligands can improve gas adsorption capacity by grafting polar functional groups. Significantly, the transformation of ligand bodies (benzene ring, triazole, urea group) and the introduction of functional groups (−NO_2, −NH_2, −CH_3, and −F) in isostructural PMOF[23−26] can effectively regulate the pore environment engineering and achieve efficient gas storage and purification.

Received: June 2, 2024
Revised: July 24, 2024
Accepted: July 25, 2024
Published: July 30, 2024

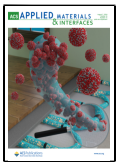

Scheme 1. Conceptual Optimized of Three PMOFs Constructed by V-Type Tetracarboxylate Linkers and Copper Paddlewheel

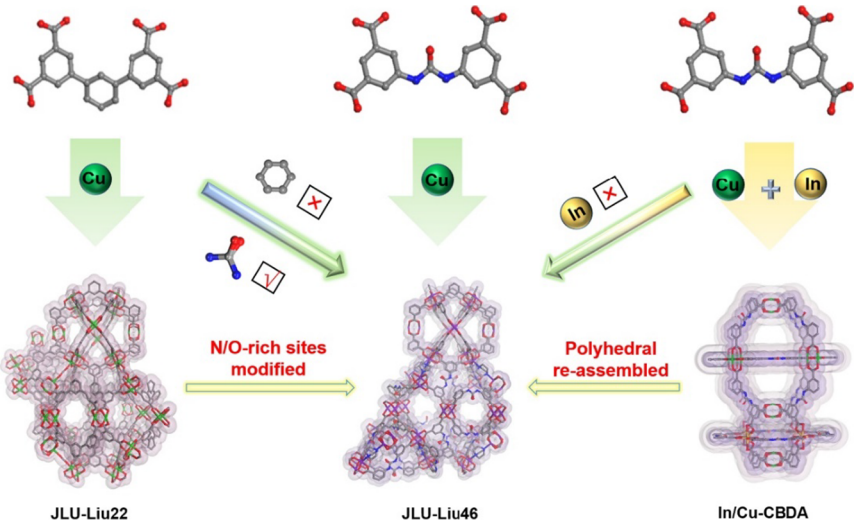

Combined with the previous work of our research group, we carefully selected a class of PMOFs based on V-type tetracarboxylic acid linker and further discussed the influence of pore environment engineering on C_2H_2 purification. The diversity of polyhedral cages in their structures provides a platform for further in-depth research on the influence of pore environment engineering on gas adsorption and separation (Scheme 1). As anticipated, all three materials exhibited high C_2H_2 adsorption capacity in ternary C_2 gas. **JLU-Liu46** demonstrated superior performance in the separation and purification of C_2H_2 compared with the other two adsorbents. Grand Canonical Monte Carlo (GCMC) simulations have demonstrated that C_2H_2 displays high adsorption and selectivity among the three PMOFs due to its strong interaction with the Cu site and multiple hydrogen bondings. Furthermore, transient breakthrough simulations of the selected samples confirmed their potential for separating C_2H_2 in ternary C_2 gas.

EXPERIMENTAL SECTION

Materials and Measurements. All chemical materials were purchased from commercial sources and required unnecessary further purification. Powder X-ray diffraction (PXRD) data were carried on a Rigaku D/max-2550 diffractometer with Cu Kα radiation (λ = 1.5418 Å). Gas adsorption and desorption isotherms were measured on a Quantachrome autosorb iQ. Thermogravimetric analysis (TGA) was performed on a Netzsch TG209F3 thermogravimetric with a temperature range of 25−800 °C, an air atmosphere, and an airflow heating rate of 10 °C min^{-1}.

Preparation of Compounds. The detailed procedure for the synthesis of **JLU-Liu22**,[27] **JLU-Liu46**,[28] and **In/Cu-CBDA**[29] could be found in Liu group and our recently reported work (see the Supporting Information)

RESULTS AND DISCUSSION

Structural Description of Compounds. The synthesis of three compounds was successfully achieved, and the obtained PXRD data exhibited excellent agreement with the reported structural simulation model, thereby confirming their exceptional crystallinity and purity (Figure S1). Meanwhile, TGA also confirmed the robustness of the materials. From the perspective of the TGA curve of **JLU-Liu46**, the initial weight losses before 250 °C correspond to guest solvents inside the pore followed by a plateau. Subsequently, the framework collapsed with the temperature rise (Figure S2). As depicted in Figure 1, **JLU-Liu22** and **JLU-Liu46** are interconnected through typical copper paddlewheel and tetracarboxylic acid ligands, thus establishing identical topology-based isoreticular (fcu). Differently, on the one hand, the two ligands encompass distinct functional groups: benzene and urea, respectively. On the other hand, the bridge ligand of paddlewheels in **JLU-Liu22** is HCOOH produced by the decomposition of the solvent DMF, while **JLU-Liu46** is the added DABCO raw material. It results in the distance between paddlewheels in **JLU-Liu22** (6.1 Å) slightly smaller than that of **JLU-Liu46** (6.9 Å) (Figure S3). Moreover, based on **JLU-Liu46**, the heterometallic PMOF **In/Cu-CBDA** was obtained by introducing saturated coordinated mononuclear indium. Among them, **JLU-Liu22** and **JLU-Liu46** possess three cage types: cuboctahedron (cuo), truncated octahedron (T-O_h), and truncated tetrahedron (T-T_d). **In/Cu-CBDA** contains two cage types: an octahedron and a slender octahedron. Overall, a powerful strategy was employed for all three compounds, including the classical scaffolding setup of polyhedral-based cage MOFs.

Gas Adsorption and Separation. The intriguing pore environment and well-developed porosity may result in excellent gas adsorption performance, which prompted us to systematically investigate the relationship between the structure of MOF materials and the C_2 gas adsorption. First, the CO_2 adsorption amounts of them are consistent with that reported in the literature[27−29] at 273 K, indicating that the activation treatment of these three as-synthesized has been well done (Figure S4). Then, the single-component adsorption performances of compounds for C_2H_2, C_2H_4, and C_2H_6 were measured at 273 and 298 K under 1 atm (Figures 2a−c and S5−S7). The uptake of **JLU-Liu22** for C_2H_2 is 237.6 and 163.5 cm^3 g^{-1}, C_2H_4 is 172 and 124.7 cm^3 g^{-1}, and C_2H_6 is 173 and 121.9 cm^3 g^{-1}, respectively. The uptakes of **JLU-Liu46** for C_2H_2 is 228 and 153.9 cm^3 g^{-1}, C_2H_4 is 151.2 and 113.6 cm^3 g^{-1}, C_2H_6 is 156.8 and 109.4 cm^3 g^{-1}, respectively. It is noted that the C_2H_2 uptake capacity of both of them at 273 K is remarkably high, which is higher than those of most renowned MOFs, such as FJU-90[30] (216 cm^3 g^{-1}), HKUST-1[31] (201 cm^3 g^{-1}), and MOF-505[32] (177 cm^3 g^{-1}). At 298 K, the C_2H_2

https://doi.org/10.1021/acsami.4c09066
ACS Appl. Mater. Interfaces 2024, 16, 41542−41550

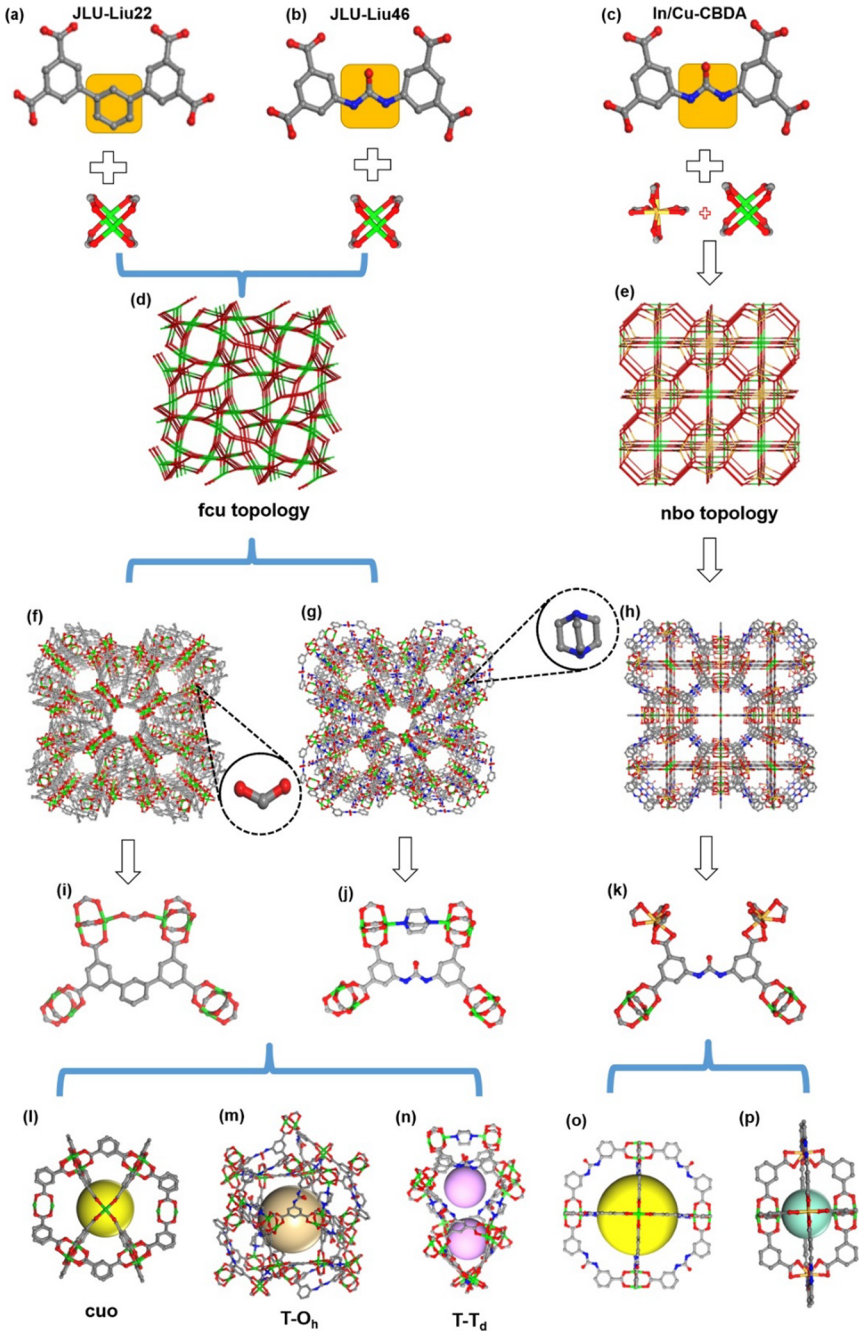

Figure 1. Description of the crystallographic structure of compounds: (a–c) secondary building units; (d, e) topology networks; (f–h) ball–stick model of the 3D framework; (i–k) three paddlewheels; (l–p) several types of polyhedron-based cage.

absorbed amounts of both can be higher than 150 $cm^3\ g^{-1}$, which is superior to those of most benchmark materials (Figure 2d) and especially V-tetracarboxylic acid noncage MOFs (ZJNU-55,[33] 56.3 $cm^3\ g^{-1}$). **In/Cu-CBDA** exhibits high adsorption capacities to C_2H_2 (137.6/80 $cm^3\ g^{-1}$), C_2H_4 (91/43 $cm^3\ g^{-1}$) and C_2H_6 (107/65 $cm^3\ g^{-1}$) at 273/298 K. As a whole, the C_2H_2 absorption capacity of all MOFs is significantly higher than C_2H_4 and C_2H_6, especially in the low-pressure range (0.1 bar) at 298 K (Figure 3a–c), which may be due to the enhanced generation of OMSs contribute to the preferential adsorption of unsaturated hydrocarbons, while the urea group's N/O site acts as an organic hydrogen bond receptor, thereby augmenting the host–guest affinity and resulting in a more robust interaction between the framework and C_2H_2.

In order to evaluate the affinity between host and guest, the Q_{st} of various gas molecules was obtained according to the Viral method based on the adsorption isotherms at 298 and 273 K. (Figures 2e,f, S8, and S9). Gas adsorption isotherms were fitted with the two-locus Langmuir–Freundlich (DSLF) equation. As shown in Figure 2e, at zero coverage, the Q_{st} values of **JLU-Liu22**, **JLU-Liu46**, and **In/Cu-CBDA** are 36, 41, and 38 kJ mol^{-1} for C_2H_2, 35, 21, and 29 kJ mol^{-1} for C_2H_4, and 39, 31, and 29 kJ mol^{-1} for C_2H_6, respectively. Their Q_{st} values of C_2H_2 higher than those of most reported MOF materials, such as JNU-1[34] (13 kJ mol^{-1}), UPC-200(Fe)-F-BIM-15[35] (20.5 kJ mol^{-1}), and MUF-15[36] (24.5 kJ

https://doi.org/10.1021/acsami.4c09066
ACS Appl. Mater. Interfaces 2024, 16, 41542–41550

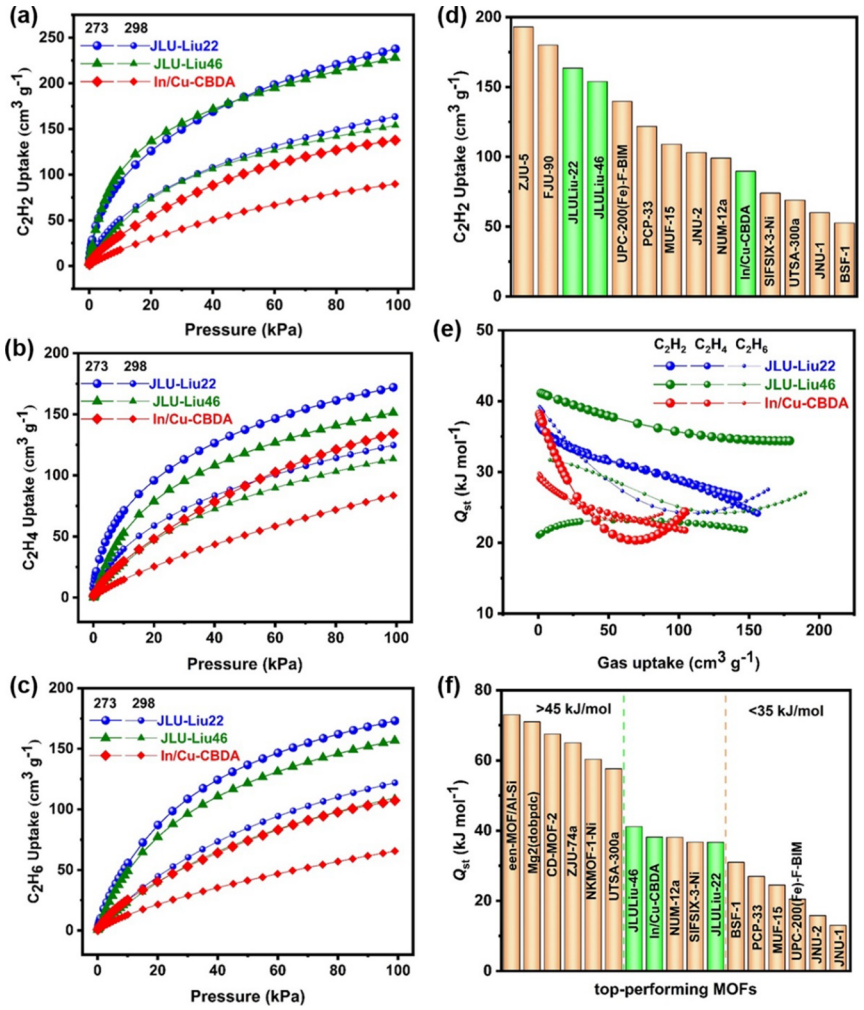

Figure 2. (a–c) Single-component adsorption isotherms of C_2H_2, C_2H_4, and C_2H_6 at 298 K under 1 atm (desorption points are removed for clarity); (d) comparison of advanced materials for C_2H_2 uptake at 1 and 298 K; (e) Q_{st} of compounds for C_2H_2, C_2H_4, and C_2H_6; and (f) comparison of advanced materials for Q_{st} at 1 atm and 298 K.

mol^{-1}), and slightly lower than those for ZJU-74a[1] (65 kJ mol^{-1}), NKMOF-1-Ni[12] (60.3 kJ mol^{-1}), and UTSA-300a[37] (57.6 kJ mol^{-1}) (Figure 2f and Table S2). It is worth noting that the Q_{st} values of C_2H_2 for **JLU-Liu46** and **In/Cu-CBDA** at zero coverage are higher than that of C_2H_4 and C_2H_6, indicating that the interaction between the C_2H_2 molecule and the framework is the strongest. For **JLU-Liu22**, the abnormally high Q_{st} of C_2H_6 can be attributed to the low polarity of the benzene ring in the framework enhanced its interaction with C_2H_6 molecules.[38] As we all know, MOFs with Q_{st} between 35 and 45 kJ/mol are relatively energy-efficient for desorption materials.[39] Generally speaking, their moderately high Q_{st} values not only confirm the strong affinity for C_2H_2 adsorption but also allow a relatively lower energy penalty of regeneration.

To evaluate the separation performance for the three compounds, the adsorption selectivity of the three compounds to the mixture of 298 K and 100 kPa was calculated using the ideal adsorption solution theory (IAST), and the refined parameters for the dual-site Langmuir–Freundlich equations were given (Tables S3–S5). As displayed in Figure 3d, the selectivity of C_2H_2/C_2H_4 and C_2H_2/C_2H_6 (50/50, v/v) was calculated to be 1.63/2.48, 2.06/2.43, and 1.22/1.60 on **JLU-Liu22**, **JLU-Liu46**, and **In/Cu-CBDA**, respectively, indicating that the material is more likely to adsorb C_2H_2 than C_2H_4 and C_2H_6. Simultaneously, the selectivity of C_2H_2/CO_2 is also calculated, taking into account that CO_2 serves as the primary impurity in acetylene production (Figure S10c). Apparently, the selectivity of **JLU-Liu22** and **JLU-Liu46** are comparable to previously reported adsorbent materials like BSF-1[40] under the same conditions, exceeding that of most reported high acetylene adsorption MOFs (Figure 3e).[1,12,41−51] It is worth noting that **JLU-Liu46** showed the best performance in the separation and purification of acetylene. The phenomena can be mainly attributed to pore environment engineering, the urea group[52] can sever as hydrogen bond acceptors to form multiple interactions, and the high-density OMSs[53−56] can give π-interactions with C_2H_2 (formation of metal–alkyne complexes), which is beneficial to its gas adsorption and separation. To test the excellent recyclability and easy regeneration of compounds, repeated adsorption and desorption experiments were performed, and the results showed that it can maintain adsorption performance almost without losing the absorption of C_2H_2 (Figures 3f and S11), and the PXRD pattern of the sample after the cycling test further confirmed the stability (Figure S1).

Transient Breakthrough Simulations. To evaluate the gas separation performance of **JLU-Liu46**, the transient breakthrough simulation of an equimolar two-component

https://doi.org/10.1021/acsami.4c09066
ACS Appl. Mater. Interfaces 2024, 16, 41542−41550

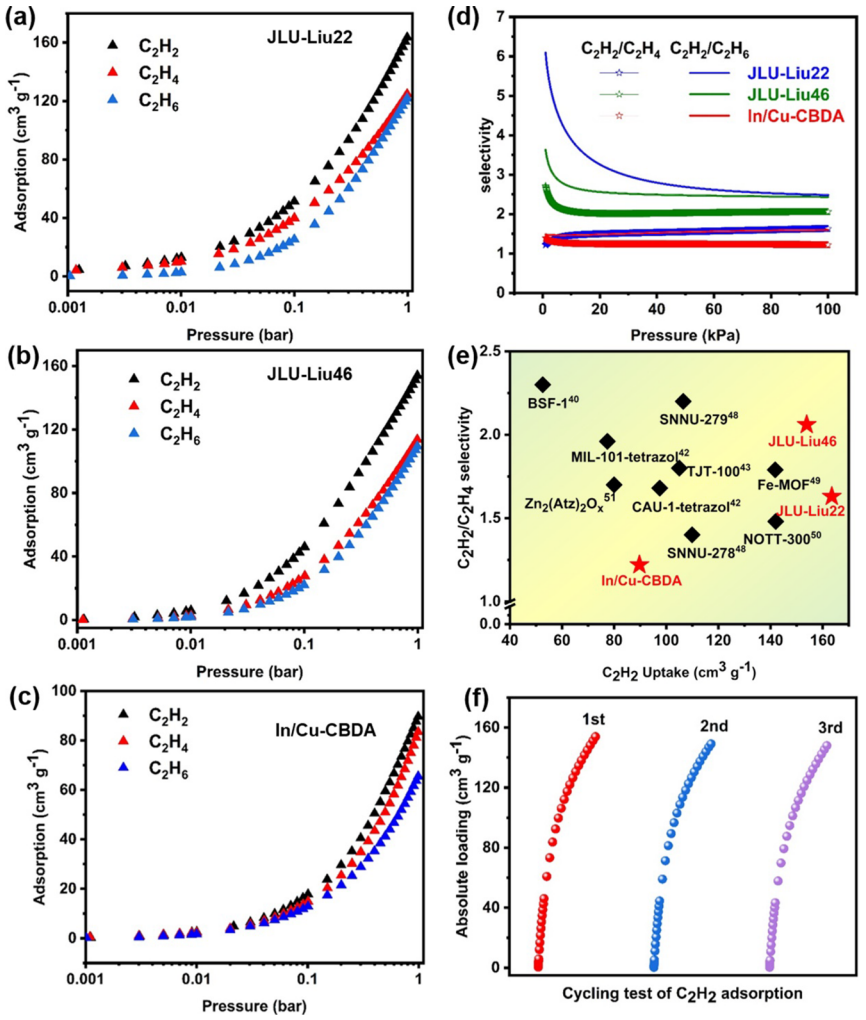

Figure 3. (a–c) C_2H_2, C_2H_4, and C_2H_6 steepness of the adsorption curve at low pressure for compounds; (d) C_2H_2/C_2H_4 and C_2H_2/C_2H_6 adsorption selectivity are predicted by IAST at 298 K and 1 atm for compounds (e) comparison of advanced materials for C_2H_2/C_2H_6 selectivity at 1 atm and 298 K; and (f) repetitive C_2H_2 adsorption measurements of **JLU-Liu46** at 298 K.

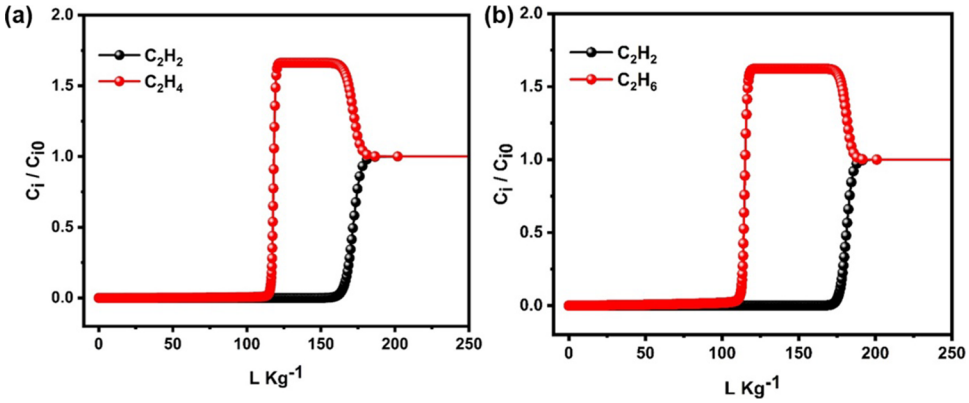

Figure 4. Simulations of transient breakthrough characteristics for **JLU-Liu46** at 100 kPa and 298 K; (a) and (b) equimolar two-component C_2H_2/C_2H_4 and C_2H_2/C_2H_6 mixture.

C_2H_2/C_2H_4 and C_2H_2/C_2H_6, as well as three-component $C_2H_2/C_2H_4/C_2H_6$ mixture operating, were investigated at a total pressure of 100 kPa and 298 K in a fixed bed packed with **JLU-Liu46**. In transient breakthrough experiments, the gas phase concentrations can be monitored only at the exit of the adsorbent. Therefore, for the presentation of the results of the breakthrough simulations, the *x*-axis presents in terms of L kg^{-1}; the *y*-axis represents the dimensionless concentration of the components at the exit of the fixed bed adsorbent. As shown in Figures 4 and S12, efficient separation was observed, where C_2H_6 and C_2H_4 breakthrough occurred first and after a certain time C_2H_2 breakthrough was observed, indicating that **JLU-Liu46** has the potential to separate C_2H_2 from C_2 gas.

https://doi.org/10.1021/acsami.4c09066
ACS Appl. Mater. Interfaces 2024, 16, 41542–41550

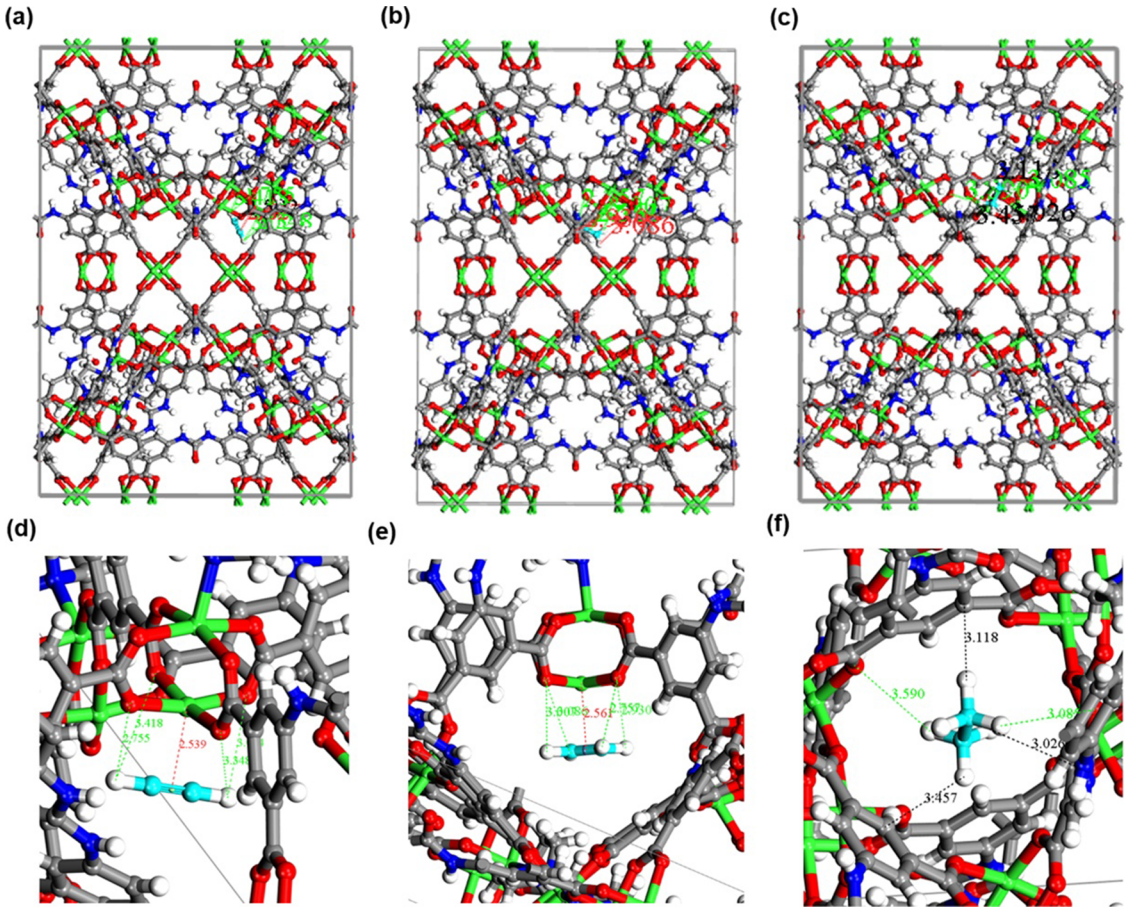

Figure 5. Simulation snapshot for (a) C_2H_2, (b) C_2H_4, and (c) C_2H_6 molecules under 298 K and 100 kPa in the **JLU-Liu46**; (d–f) represents an enlarged depiction of the molecular simulation snapshots for C_2H_2, C_2H_4, and C_2H_6.

GCMC Simulations. To gain precise insight into the preferential adsorption sites of C_2H_2, C_2H_4, and C_2H_6 in **JLU-Liu46**, molecular modeling was performed based on GCMC simulations. The C_2H_2 molecule exhibits a strong interaction force with the Cu site at a short distance of 2.539 Å, and forms interactions with four carboxylate O atoms through C−H···O hydrogen bonds (H···O = 2.775−3.418 Å) (Figure 5a,d). In the case of C_2H_4, it interacts with the Cu site at 2.561 Å distance and involves multiple C−H···O hydrogen bonds (H···O = 2.757−3.086 Å). (Figure 5b,e). In comparison, C_2H_6 gas molecules were preferentially located at the cavities built by three $[Cu_2(COO)_4]$ paddlewheel and three tetracarboxylate linkers, the framework and C_2H_6 molecules only form multiple C−H···π interaction and C−H···O/N hydrogen bonds (H···O/N = 3.026−3.590 Å) (Figure 5c, f). Therefore, the MOF possesses a greater affinity for C_2H_2 relative to those for C_2H_4 and C_2H_6. Meanwhile, the density distribution also showed C_2H_2 molecules in **JLU-Liu46** are apparently higher than C_2H_4 and C_2H_6 (Figure S13).

CONCLUSIONS

The search for optimal adsorbents capable of one-step separation of C_2H_2 from $C_2H_6/C_2H_4/C_2H_2$ mixtures represents an important but challenging task in the industry. In this work, we investigated the C_2 adsorption and separation performance of three PMOFs with similar cage-based structures and systematically studied the effects of functional groups and OMSs. Compared with the other two adsorbents, **JLU-Liu46** showed the best performance in the separation and purification of acetylene. This relatively high selectivity of C_2H_2 is attributed to the synergistic effects arising from coordinatively unsaturated Cu sites combined with an optimal pore environment (matched pore size and polarity, urea functional group), which can enhance the affinity of the adsorbate and adsorbent. Transient breakthrough simulations with ternary and binary C_2 gas mixtures confirmed the ability of **JLU-Liu46** to effectively separate C_2H_2. In addition, the persistent reusability of **JLU-Liu46** in C_2 separation was confirmed by multicycle experiments. Our study may provide valuable insight for future development of ideal adsorbents for the adsorptive purification of C_2H_2.

ASSOCIATED CONTENT

Supporting Information

The Supporting Information is available free of charge at https://pubs.acs.org/doi/10.1021/acsami.4c09066.

PXRD, as-synthesized and activated samples of TGA curves, center distance of the terminal benzenes, CO_2 adsorption and desorption isotherms, fitting results, repetitive C_2H_2 adsorption measurements, simulations of transient breakthrough characteristics curves, density distribution, and calculation procedures of Q_{st} and selectivity from IAST (PDF)

https://doi.org/10.1021/acsami.4c09066
ACS Appl. Mater. Interfaces 2024, 16, 41542−41550

AUTHOR INFORMATION

Corresponding Author

Dongmei Wang − *Key Laboratory of the Ministry of Education for Advanced Catalysis Materials, College of Chemistry and Materials Sciences, Zhejiang Normal University, Jinhua 321004, P.R. China;* orcid.org/0000-0002-8221-7144; Email: dmwang@zjnu.edu.cn

Authors

Xia Zhou − *Key Laboratory of the Ministry of Education for Advanced Catalysis Materials, College of Chemistry and Materials Sciences, Zhejiang Normal University, Jinhua 321004, P.R. China*

Zitong Song − *Key Laboratory of the Ministry of Education for Advanced Catalysis Materials, College of Chemistry and Materials Sciences, Zhejiang Normal University, Jinhua 321004, P.R. China*

Rajamani Krishna − *Van't Hoff Institute for Molecular Sciences, University of Amsterdam, Amsterdam 1090 GE, Nederland;* orcid.org/0000-0002-4784-8530

Lixiaoxiao Shi − *Key Laboratory of the Ministry of Education for Advanced Catalysis Materials, College of Chemistry and Materials Sciences, Zhejiang Normal University, Jinhua 321004, P.R. China*

Kangli Zhang − *Key Laboratory of the Ministry of Education for Advanced Catalysis Materials, College of Chemistry and Materials Sciences, Zhejiang Normal University, Jinhua 321004, P.R. China*

Complete contact information is available at: https://pubs.acs.org/10.1021/acsami.4c09066

Notes

The authors declare no competing financial interest.

ACKNOWLEDGMENTS

This work was supported by the National Natural Science Foundation of China (52102189) and Jinhua City Project (2023-4-019).

REFERENCES

(1) Pei, J.; Shao, K.; Wang, J. X.; Wen, H. M.; Yang, Y.; Cui, Y.; Krishna, R.; Li, B.; Qian, G. A Chemically Stable Hofmann-Type Metal-Organic Framework with Sandwich-Like Binding Sites for Benchmark Acetylene Capture. *Adv. Mater.* **2020**, *32* (24), No. e1908275.

(2) Zhang, Q.; Zhou, L.; Liu, P.; Li, L.; Yang, S.-Q.; Li, Z.-F.; Hu, T.-L. Integrating Tri-Mural Nanotraps into a Microporous Metal-Organic Framework for C_2H_2/CO_2 and C_2H_2/C_2H_4 Separation. *Sep. Purif. Technol.* **2022**, *296*, No. 121404.

(3) Fu, X.-P.; Wang, Y.-L.; Zhang, X.-F.; Krishna, R.; He, C.-T.; Liu, Q.-Y.; Chen, B. Collaborative Pore Partition and Pore Surface Fluorination within a Metal−Organic Framework for High-Performance C_2H_2/CO_2 Separation. *Chem. Eng. J.* **2022**, *432*, No. 134433.

(4) Hua, G. F.; Xie, X. J.; Lu, W.; Li, D. Optimizing Supramolecular Interactions in Metal-Organic Frameworks for C_2 Separation. *Dalton Trans.* **2020**, *49* (44), 15548−15559.

(5) Schobert, H. Production of Acetylene and Acetylene-Based Chemicals from Coal. *Chem. Rev.* **2014**, *114* (3), 1743−1760.

(6) Trotus, I. T.; Zimmermann, T.; Schuth, F. Catalytic Reactions of Acetylene: A Feedstock for the Chemical Industry Revisited. *Chem. Rev.* **2014**, *114* (3), 1761−1782.

(7) Ding, Q.; Zhang, Z.; Liu, Y.; Chai, K.; Krishna, R.; Zhang, S. One-Step Ethylene Purification from Ternary Mixtures in a Metal-Organic Framework with Customized Pore Chemistry and Shape. *Angew. Chem., Int. Ed. Engl.* **2022**, *61* (35), No. e202208134.

(8) Jiang, X.; Wang, Y.; Cao, J. W.; Ye, Z. M.; Zhang, T.; Liu, D. X.; Li, K. L.; Yang, R.; Wang, T.; Zhang, Q. Y.; Chen, K. J. Low-Concentration C_2H_6 Capture Enabled by Size Matching in the Ultramicropore. *Chem. - Eur. J.* **2021**, *27* (50), 12753−12757.

(9) Ma, L. L.; An, N.; Guo, F. A.; Wang, H.; Yang, G. P.; Wang, Y. Y. Separation of $C_2H_2/C_2H_4/C_2H_6$ and C_2H_2/CO_2 in a Nitrogen-Rich Copper-Based Microporous Metal-Organic Framework. *Inorg. Chem.* **2023**, *62* (34), 13698−13701.

(10) Di, Z.; Zheng, X.; Qi, Y.; Yuan, H.; Li, C.-P. Recent Advances in C_2 Gases Separation and Purification by Metal-Organic Frameworks. *Chin. J. Struct. Chem.* **2022**, *41*, 2211031−2211044.

(11) Zhang, L.; Xiao, T.; Zeng, X.; You, J.; He, Z.; Chen, C. X.; Wang, Q.; Nafady, A.; Al-Enizi, A. M.; Ma, S. Isoreticular Contraction of Cage-Like Metal-Organic Frameworks with Optimized Pore Space for Enhanced C_2H_2/CO_2 and C_2H_2/C_2H_4 Separations. *J. Am. Chem. Soc.* **2024**, *146* (11), 7341−7351.

(12) Peng, Y. L.; Pham, T.; Li, P.; Wang, T.; Chen, Y.; Chen, K. J.; Forrest, K. A.; Space, B.; Cheng, P.; Zaworotko, M. J.; Zhang, Z. Robust Ultramicroporous Metal-Organic Frameworks with Benchmark Affinity for Acetylene. *Angew. Chem., Int. Ed. Engl.* **2018**, *57* (34), 10971−10975.

(13) Cui, W. G.; Hu, T. L.; Bu, X. H. Metal-Organic Framework Materials for the Separation and Purification of Light Hydrocarbons. *Adv. Mater.* **2020**, *32* (3), No. e1806445.

(14) Tan, Y. X.; Lin, J.; Li, Q. H.; Li, L.; Borse, R. A.; Lu, W.; Wang, Y.; Yuan, D. Overcoming the Trade-Off between C_2H_2 Sorption and Separation Performance by Regulating Metal-Alkyne Chemical Interaction in Metal-Organic Frameworks. *Angew. Chem., Int. Ed. Engl.* **2023**, *62* (22), No. e202302882.

(15) Hu, Y.; Jiang, Y.; Li, J.; Wang, L.; Steiner, M.; Neumann, R. F.; Luan, B.; Zhang, Y. New-Generation Anion-Pillared Metal−Organic Frameworks with Customized Cages for Highly Efficient CO_2 Capture. *Adv. Funct. Mater.* **2023**, *33* (14), No. 2213915.

(16) Gao, C.; Mu, X.-B.; Yuan, W.-Y.; Zhang, P.; Wang, Y.; Zhai, Q.-G. Construction of New Multi-Cage-Based Mofs Using Flexible Triangular Ligands for Efficient Gas Adsorption and Separation. *J. Solid State Chem.* **2023**, *322*, No. 123994.

(17) Li, H.; Liu, C.; Chen, C.; Di, Z.; Yuan, D.; Pang, J.; Wei, W.; Wu, M.; Hong, M. An Unprecedented Pillar-Cage Fluorinated Hybrid Porous Framework with Highly Efficient Acetylene Storage and Separation. *Angew. Chem., Int. Ed. Engl.* **2021**, *60* (14), 7547−7552.

(18) Lin, X.; Telepeni, I.; Blake, A. J.; Dailly, A.; Brown, C. M.; Simmons, J. M.; Zoppi, M.; Walker, G. S.; Thomas, K. M.; Mays, T. J.; Hubberstey, P.; Champness, N. R.; Schröder, M. High Capacity Hydrogen Adsorption in Cu(II) Tetracarboxylate Framework Materials: The Role of Pore Size, Ligand Functionalization, and Exposed Metal Sites. *J. Am. Chem. Soc.* **2009**, *131* (6), 2159−2171.

(19) Yan, Y.; Juricek, M.; Coudert, F. X.; Vermeulen, N. A.; Grunder, S.; Dailly, A.; Lewis, W.; Blake, A. J.; Stoddart, J. F.; Schroder, M. Non-Interpenetrated Metal-Organic Frameworks Based on Copper(II) Paddlewheel and Oligoparaxylene-Isophthalate Linkers: Synthesis, Structure, and Gas Adsorption. *J. Am. Chem. Soc.* **2016**, *138* (10), 3371−3381.

(20) Wen, H. M.; Yu, C.; Liu, M.; Lin, C.; Zhao, B.; Wu, H.; Zhou, W.; Chen, B.; Hu, J. Construction of Negative Electrostatic Pore Environments in a Scalable, Stable and Low-Cost Metal-Organic Framework for One-Step Ethylene Purification from Ternary Mixtures. *Angew. Chem., Int. Ed.* **2023**, *62* (44), No. e202309108.

(21) Liu, B.; Yao, S.; Shi, C.; Li, G.; Huo, Q.; Liu, Y. Significant Enhancement of Gas Uptake Capacity and Selectivity Via the Judicious Increase of Open Metal Sites and Lewis Basic Sites within Two Polyhedron-Based Metal-Organic Frameworks. *Chem. Commun.* **2016**, *52* (15), 3223−3226.

(22) Lu, Z.; Xing, Y.; Du, L.; He, H.; Zhang, J.; Hang, C. Isostructural Functionalization by − OH and $-NH_2$: Different Contributions to CO_2 Adsorption. *RSC Adv.* **2017**, *7* (75), 47219−47224.

(23) Gu, X. W.; Wang, J. X.; Wu, E.; Wu, H.; Zhou, W.; Qian, G.; Chen, B.; Li, B. Immobilization of Lewis Basic Sites into a Stable

Ethane-Selective Mof Enabling One-Step Separation of Ethylene from a Ternary Mixture. *J. Am. Chem. Soc.* **2022**, *144* (6), 2614−2623.
(24) Li, P. Z.; Wang, X. J.; Zhang, K.; Nalaparaju, A.; Zou, R.; Zou, R.; Jiang, J.; Zhao, Y. "Click"-Extended Nitrogen-Rich Metal-Organic Frameworks and Their High Performance in CO_2-Selective Capture. *Chem. Commun.* **2014**, *50* (36), 4683−4685.
(25) Xie, F.; Liu, J.; Graham, W.; Ullah, S.; Moisés Cedeño Morales, E.; Tan, K.; Thonhauser, T.; Wang, H.; Li, J. The Effect of Pore Structure in Ethane-Selective Metal-Organic Frameworks for Ethylene Purification. *Chem. Eng. J.* **2023**, *473*, No. 145096.
(26) Zhang, M.; Zhao, H.; Wang, Y.; Jiang, J.; Chen, M.; He, X.; Liu, P.; Dang, R.; Cui, H.; Wang, M.; Sun, T.; Qin, G.; Tang, Y.; Wang, S. Fine-Tuning Mofs with Amino Group for One-Step Ethylene Purification from the C_2 Hydrocarbon Mixture. *Inorg. Chem.* **2023**, *62* (21), 8428−8434.
(27) Wang, D.; Liu, B.; Yao, S.; Wang, T.; Li, G.; Huo, Q.; Liu, Y. A Polyhedral Metal-Organic Framework Based on the Supermolecular Building Block Strategy Exhibiting High Performance for Carbon Dioxide Capture and Separation of Light Hydrocarbons. *Chem. Commun.* **2015**, *51* (83), 15287−15289.
(28) Liu, B.; Yao, S.; Liu, X.; Li, X.; Krishna, R.; Li, G.; Huo, Q.; Liu, Y. Two Analogous Polyhedron-Based Mofs with High Density of Lewis Basic Sites and Open Metal Sites: Significant CO_2 Capture and Gas Selectivity Performance. *ACS Appl. Mater. Interfaces* **2017**, *9* (38), 32820−32828.
(29) Wang, D.; Zhang, Y.; Gao, J.; Ge, G.; Li, C. A Polyhedron-Based Heterometallic Mof Constructed by Hsab Theory and Sbb Strategy: Synthesis, Structure, and Adsorption Properties. *Cryst. Growth Des.* **2019**, *19* (8), 4571−4578.
(30) Ye, Y.; Ma, Z.; Lin, R. B.; Krishna, R.; Zhou, W.; Lin, Q.; Zhang, Z.; Xiang, S.; Chen, B. Pore Space Partition within a Metal-Organic Framework for Highly Efficient C_2H_2/CO_2 Separation. *J. Am. Chem. Soc.* **2019**, *141* (9), 4130−4136.
(31) Xiang, S.; Zhou, W.; Gallegos, J. M.; Liu, Y.; Chen, B. Exceptionally High Acetylene Uptake in a Microporous Metal−Organic Framework with Open Metal Sites. *J. Am. Chem. Soc.* **2009**, *131* (34), 12415−12419.
(32) Chen, B.; Ockwig, N. W.; Millward, A. R.; Contreras, D. S.; Yaghi, O. M. High H_2 Adsorption in a Microporous Metal-Organic Framework with Open Metal Sites. *Angew. Chem., Int. Ed. Engl.* **2005**, *44* (30), 4745−4749.
(33) Jiao, J.; Liu, H.; Chen, F.; Bai, D.; Xiong, S.; He, Y. An Anionic Metal−Organic Framework Based on Angular Tetracarboxylic Acid and a Mononuclear Copper Ion for Selective Gas Adsorption. *Inorg. Chem. Front.* **2016**, *3* (11), 1411−1418.
(34) Zeng, H.; Xie, M.; Huang, Y. L.; Zhao, Y.; Xie, X. J.; Bai, J. P.; Wan, M. Y.; Krishna, R.; Lu, W.; Li, D. Induced Fit of C_2H_2 in a Flexible Mof through Cooperative Action of Open Metal Sites. *Angew. Chem., Int. Ed. Engl.* **2019**, *58* (25), 8515−8519.
(35) Fan, W.; Yuan, S.; Wang, W.; Feng, L.; Liu, X.; Zhang, X.; Wang, X.; Kang, Z.; Dai, F.; Yuan, D.; Sun, D.; Zhou, H. C. Optimizing Multivariate Metal-Organic Frameworks for Efficient C_2H_2/CO_2 Separation. *J. Am. Chem. Soc.* **2020**, *142* (19), 8728−8737.
(36) Qazvini, O. T.; Macreadie, L. K.; Telfer, S. G. Effect of Ligand Functionalization on the Separation of Small Hydrocarbons and CO_2 by a Series of Muf-15 Analogues. *Chem. Mater.* **2020**, *32* (15), 6744−6752.
(37) Lin, R. B.; Li, L.; Wu, H.; Arman, H.; Li, B.; Lin, R. G.; Zhou, W.; Chen, B. Optimized Separation of Acetylene from Carbon Dioxide and Ethylene in a Microporous Material. *J. Am. Chem. Soc.* **2017**, *139* (23), 8022−8028.
(38) Liu, J.; Zhou, K.; Ullah, S.; Miao, J.; Wang, H.; Thonhauser, T.; Li, J. Precise Pore Engineering of Fcu-Type Y-Mofs for One-Step C_2H_4 Purification from Ternary $C_2H_6/C_2H_4/C_2H_2$ Mixtures. *Small* **2023**, *19* (42), No. 2304460.
(39) Lou, W.; Li, J.; Sun, W.; Hu, Y.; Wang, L.; Neumann, R. F.; Steiner, M.; Gu, Z.; Luan, B.; Zhang, Y. Screening Hoffman-Type Metal Organic Frameworks for Efficient C_2H_2/CO_2 Separation. *Chem. Eng. J.* **2023**, *452*, No. 139296.
(40) Zhang, Y.; Yang, L.; Wang, L.; Duttwyler, S.; Xing, H. A Microporous Metal-Organic Framework Supramolecularly Assembled from a Cu(II) Dodecaborate Cluster Complex for Selective Gas Separation. *Angew. Chem., Int. Ed. Engl.* **2019**, *58* (24), 8145−8150.
(41) Choe, J. H.; Kim, H.; Kang, M.; Yun, H.; Kim, S. Y.; Lee, S. M.; Hong, C. S. Functionalization of Diamine-Appended Mof-Based Adsorbents by Ring Opening of Epoxide: Long-Term Stability and CO_2 Recyclability under Humid Conditions. *J. Am. Chem. Soc.* **2022**, *144* (23), 10309−10319.
(42) Fan, W.; Peh, S. B.; Zhang, Z.; Yuan, H.; Yang, Z.; Wang, Y.; Chai, K.; Sun, D.; Zhao, D. Tetrazole-Functionalized Zirconium Metal-Organic Cages for Efficient C_2H_2 /C_2H_4 and C_2H_2 /CO_2 Separations. *Angew. Chem., Int. Ed. Engl.* **2021**, *60* (32), 17338−17343.
(43) Hao, H. G.; Zhao, Y. F.; Chen, D. M.; Yu, J. M.; Tan, K.; Ma, S.; Chabal, Y.; Zhang, Z. M.; Dou, J. M.; Xiao, Z. H.; Day, G.; Zhou, H. C.; Lu, T. B. Simultaneous Trapping of C_2H_2 and C_2H_6 from a Ternary Mixture of C_2H_2 /C_2H_4 /C_2H_6 in a Robust Metal-Organic Framework for the Purification of C_2H_4. *Angew. Chem., Int. Ed. Engl.* **2018**, *57* (49), 16067−16071.
(44) Li, L.; Wang, J.; Zhang, Z.; Yang, Q.; Yang, Y.; Su, B.; Bao, Z.; Ren, Q. Inverse Adsorption Separation of CO_2/C_2H_2 Mixture in Cyclodextrin-Based Metal-Organic Frameworks. *ACS Appl. Mater. Interfaces* **2019**, *11* (2), 2543−2550.
(45) Li, Y.; Wang, X.; Yang, X.; Liu, H.; Chai, X.; Wang, Y.; Fan, W.; Sun, D. Fe-Mof with U-Shaped Channels for C_2H_2/CO_2 and C_2H_2/C_2H_4 Separation. *Inorg. Chem.* **2023**, *62* (9), 3722−3726.
(46) Liu, X.; Li, Y.; Hao, C.; Fan, W.; Liu, W.; Liu, J.; Wang, Y. Optimizing the Pore Space of a Robust Nickel−Organic Framework for Efficient C_2H_2/C_2H_4 Separation. *Inorg. Chem. Front.* **2023**, *10* (3), 824−831.
(47) McDonald, T. M.; Mason, J. A.; Kong, X.; Bloch, E. D.; Gygi, D.; Dani, A.; Crocella, V.; Giordanino, F.; Odoh, S. O.; Drisdell, W. S.; Vlaisavljevich, B.; Dzubak, A. L.; Poloni, R.; Schnell, S. K.; Planas, N.; Lee, K.; Pascal, T.; Wan, L. F.; Prendergast, D.; Neaton, J. B.; Smit, B.; Kortright, J. B.; Gagliardi, L.; Bordiga, S.; Reimer, J. A.; Long, J. R. Cooperative Insertion of CO_2 in Diamine-Appended Metal-Organic Frameworks. *Nature* **2015**, *519* (7543), 303−308.
(48) Mu, X.; Xue, Y.; Hu, M.; Zhang, P.; Wang, Y.; Li, H.; Li, S.; Zhai, Q. Fine-Tuning of Pore-Space-Partitioned Metal-Organic Frameworks for Efficient C_2H_2/C_2H_4 and C_2H_2/CO_2 Separation. *Chin. Chem. Lett.* **2023**, *34* (2), No. 107296.
(49) Yang, S.; Ramirez-Cuesta, A. J.; Newby, R.; Garcia-Sakai, V.; Manuel, P.; Callear, S. K.; Campbell, S. I.; Tang, C. C.; Schröder, M. Supramolecular Binding and Separation of Hydrocarbons within a Functionalized Porous Metal−Organic Framework. *Nat. Chem.* **2015**, *7* (2), 121−129.
(50) Zhang, P.-D.; Wu, X.-Q.; He, T.; Xie, L.-H.; Chen, Q.; Li, J.-R. Selective Adsorption and Separation of C_2 Hydrocarbons in a "Flexible-Robust" Metal−Organic Framework Based on a Guest-Dependent Gate-Opening Effect. *Chem. Commun.* **2020**, *56* (41), 5520−5523.
(51) Zhang, Q.; Yang, S. Q.; Zhou, L.; Yu, L.; Li, Z. F.; Zhai, Y. J.; Hu, T. L. Pore-Space Partition through an Embedding Metal-Carboxylate Chain-Induced Topology Upgrade Strategy for the Separation of Acetylene/Ethylene. *Inorg. Chem.* **2021**, *60* (24), 19328−19335.
(52) Fan, S. C.; Li, Y. T.; Wang, Y.; Wang, J. W.; Xue, Y. Y.; Li, H. P.; Li, S. N.; Zhai, Q. G. Amide-Functionalized Metal-Organic Frameworks Coupled with Open Fe/Sc Sites for Efficient Acetylene Purification. *Inorg. Chem.* **2021**, *60* (23), 18473−18482.
(53) Alaerts, L.; Maes, M.; van der Veen, M. A.; Jacobs, P. A.; De Vos, D. E. Metal−Organic Frameworks as High-Potential Adsorbents for Liquid-Phase Separations of Olefins, Alkylnaphthalenes and Dichlorobenzenes. *Phys. Chem. Chem. Phys.* **2009**, *11* (16), 2903−2911.
(54) Lin, Z.-J.; Mahammed, S. A. R.; Liu, T.-F.; Cao, R. Multifunctional Porous Hydrogen-Bonded Organic Frameworks:

https://doi.org/10.1021/acsami.4c09066
ACS Appl. Mater. Interfaces 2024, 16, 41542−41550

Current Status and Future Perspectives. *ACS Central Science* **2022**, *8* (12), 1589−1608.
(55) Luna-Triguero, A.; Vicent-Luna, J. M.; Madero-Castro, R. M.; Gomez-Alvarez, P.; Calero, S. Acetylene Storage and Separation Using Metal-Organic Frameworks with Open Metal Sites. *ACS Appl. Mater. Interfaces* **2019**, *11* (34), 31499−31507.
(56) Zhang, Z.; Peh, S. B.; Wang, Y.; Kang, C.; Fan, W.; Zhao, D. Efficient Trapping of Trace Acetylene from Ethylene in an Ultramicroporous Metal-Organic Framework: Synergistic Effect of High-Density Open Metal and Electronegative Sites. *Angew. Chem., Int. Ed. Engl.* **2020**, *59* (43), 18927−18932.

https://doi.org/10.1021/acsami.4c09066
ACS Appl. Mater. Interfaces 2024, 16, 41542−41550

Three Polyhedron-Based Metal-Organic Frameworks Exhibiting Excellent Acetylene Selective Adsorption

Xia Zhou ,[a†] Zitong Song ,[a†] Rajamani Krishna ,[b‡] Lixiaoxiao Shi ,[a†] Kangli Zhang ,[a†] and Dongmei Wang[*,a†]

[†]Key Laboratory of the Ministry of Education for Advanced Catalysis Materials, College of Chemistry and Materials Sciences, Zhejiang Normal University, Jinhua 321004 P.R. China

[‡]Van 't Hoff Institute for Molecular Sciences University of Amsterdam, Science Park 904, Amsterdam 1090 GE, Nederland

[*]E-mail: dmwang@zjnu.edu.cn

Content

Materials and Synthesize Methods

1.1 Synthesize of JLU-Liu22[1]

A mixture of $Cu(NO_3)_2 \cdot 3H_2O$ (8 mg, 0.033 mmol), H_4tpta (2 mg, 0.005 mmol), N, N-dimethylacetamide (DMA) (1 mL), H_2O (0.65 mL), 0.65 mL of HNO_3 (2.7 M in DMF) was sealed in a glass bottle and then heated in the oven at 85 °C for 24 hours and then 105 °C for 12 h. The mixture was then cooled to room temperature. Bright-blue block crystals were obtained and air-dried (yield 60%, based on H_4tpta).

1.2 Synthesize of JLU-Liu46[2]

A mixture of $Cu(BF_4)_2 \cdot 6H_2O$ (7.5 mg, 0.012 mmol), H_4L (2 mg, 0.005 mmol), 1,4-diazabicyclo[2.2.2]-octane (DABCO) (0.1 mL, 2 g in 10 mL DMF), N,N-dimethylformamide (DMF) (1 mL), ethanol (0.5 mL), H_2O (0.5 mL), and 0.35 mL of HNO_3 (2.7 M in DMF) was sealed in a glass bottle and then heated in the oven at 85 °C for 12 h. Blue crystals were gathered, washed with DMF, and air-dried (58% yield based

on $Cu(BF_4)_2 \cdot 6H_2O$).

1.3 Synthesize of In/Cu-CBDA[3]

The mixture of $In(NO_3)_3 \cdot 4H_2O$ (10 mg, 0.03 mmol), $Cu(NO_3)_3 \cdot 3H_2O$ (8 mg, 0.03 mmol), H_4L (4 mg, 0.01 mmol), N,N-dimethylacetamide (DMA, 0.5 mL), N-methylformamide (NMF, 0.5 mL), deionized water (H_2O, 0.5 mL) and 0.35 mL of HNO_3 (2.7 M in DMA) was sealed in a glass bottle and then heated in the oven at 90 °C for 24 h. After finishing this series of operations, the blue block-shaped crystals of In/Cu-CBDA were collected, washed with fresh DMF, and airdried (yield: 73%, based on CBDA).

Gas Sorption Measurements

Gas sorption and desorption isotherms were measured on an Autosrob iQ. Before adsorption measurements, to remove all the guest solvents in the frameworks. The collected **JLU-Liu22** was washed with DMA several times, and then were first solvent-exchanged with dry ethanol at least three days. **JLU-Liu46** was washed with DMF several times and replaced with absolute ethanol (12 cycles for 3 days). The as-synthesized **In/Cu-CBDA**, washed with fresh DMA, and then were solvent-exchanged with dry acetone at least three days. Then, **JLU-Liu46**, **JLU-Liu22** and **In/Cu-CBDA** were activated under a dynamic vacuum at 373K for 10 h, respectively, which was used for gas adsorption tests.

Adsorption Enthalpy Calculation

The C_2H_2, C_2H_4 and C_2H_6 adsorption enthalpy (Q_{st}) of **JLU-Liu22**, **JLU-Liu46** and **In/Cu-CBDA** were calculated using adsorption data at 273 K and 298 K. A virial-type expression (eqn S1) was used to fit these data, and then the Q_{st} was then calculated by the expression given by eqn S2.

$$\ln P = \ln N + \frac{1}{T}\sum_{i=0}^{m} a_i N^i + \sum_{i=0}^{n} b_i N^i \qquad \text{eqn (S1)}$$

$$Q_{st} = -R\sum_{i=0}^{m} a_i N^i \qquad \text{eqn (S2)}$$

Here, *P*, *N*, and *T* are the pressure (mmHg), amount adsorbed (mmol g $^{-1}$), and temperature (K), respectively. m and n determine the number of terms required to adequately describe the isotherm. a_i and b_i are virial coefficients.

Calculation procedures of selectivity from IAST

The measured experimental data is excess loadings (q^{ex}) of the pure components C_2H_2, C_2H_4 and C_2H_6 for **JLU-Liu22**, **JLU-Liu46**and **In/Cu-CBDA**, which should be converted to absolute loadings (q) firstly.

$$q = q^{ex} + \frac{pV_{pore}}{ZRT} \qquad \text{eqn (S3)}$$

Here *Z* is the compressibility factor. The Peng-Robinson equation was used to estimate the value of compressibility factor to obtain the absolute loading, while the measure pore volume is also necessary.

In order to perform the IAST calculations, the single-component isotherm was fitted by the dual-site Langmuir-Freundlich (DSLF) adsorption model to correlate the pure-component equilibrium data and further predict the adsorption of mixtures. The DSLF model is described as:

$$q = q_{m_1} \times \frac{b_1 \times p^{1/n_1}}{1 + b_1 \times p^{1/n_1}} + q_{m_2} \times \frac{b_2 \times p^{1/n_2}}{1 + b_2 \times p^{1/n_2}} \qquad \text{eqn (S4)}$$

$$S_{ij} = \frac{x_1/x_2}{y_1/y_2} \qquad \text{eqn (S5)}$$

Here p is the pressure of the bulk gas at equilibrium with the adsorbed phase (kPa), q is the adsorbed amount per mass of adsorbent (mol kg^{-1}), q_{m1} and q_{m2} are the saturation capacities of sites 1 and 2 (mol kg^{-1}), b_1 and b_2 are the affinity coefficients of sites 1 and 2 (1/kPa), n_1 and n_2 are the deviations from an ideal homogeneous surface. To investigate the separation of binary mixtures, the adsorption selectivity is defined by x_1 and x_2 are the component loadings of the adsorbed phase in the mixture.

Transient breakthrough simulations

Transient breakthrough simulations were performed for 33.33/33.33/33.33 $C_2H_2/C_2H_4/C_2H_6$, 50/50 C_2H_2/C_2H_4, and 50/50 C_2H_2/C_2H_6 mixtures in **JLU-Liu46**

operating at 100 kPa and 298 K , using the methodology described in earlier publications[4-6] For the breakthrough simulations, the following parameter values were used: length of packed bed, L = 0.3 m; voidage of packed bed, ε = 0.4; volumetric flow rate at the entrance to the bed, Q_0 = 40 L s^{-1}

Grand Canonical Monte Carlo (GCMC) Simulations

Metropolis Monte Carlo method[7] in Sorption module of Materials Studio (MS) 2020 was employed to investigate the sorption behaviors of C_2H_2, C_2H_4 and C_2H_6 molecule upon MOF of **JLU-Liu46**. The interaction analysis included density field distribution and isosteric heat. In present sorption process, the well-known Metropolis algorithm was used to accept or reject a configurational move of considered molecules. The Berendsen thermostat was used for temperature control. 1000000 steps of Metropolis Monte Carlo calculations were carried out with the initial equilibration period of 100000 steps.

S1. Supporting Figurers

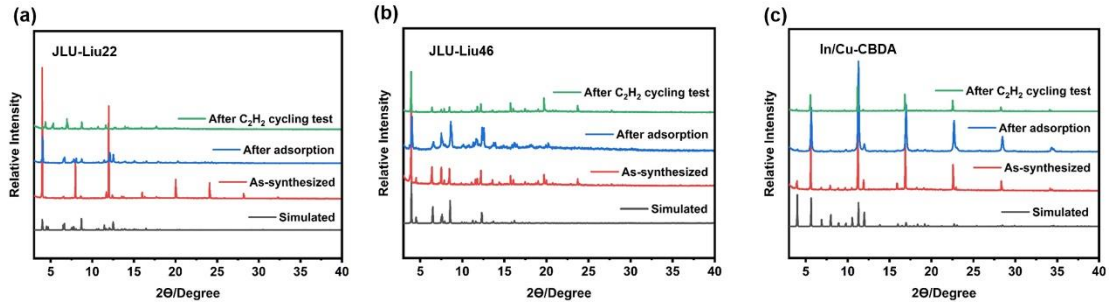

Figure S1. Simulated, as-synthesized, activated-sample and after C_2H_2 cycling test PXRD patterns of (a) **JLU-Liu22**, (b) **JLU-Liu46** and (c) **In/Cu-CBDA**.

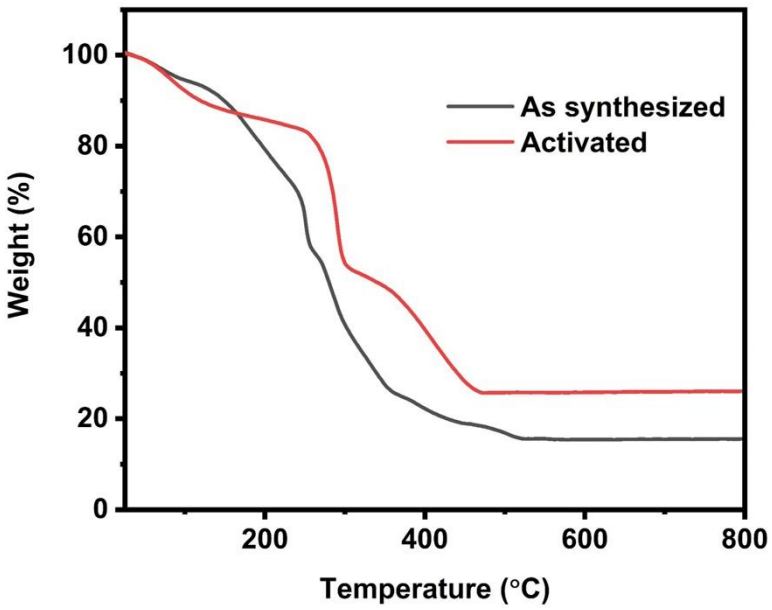

Figure S2. The as-synthesized and activated samples of TGA curves of **JLU-Liu46**.

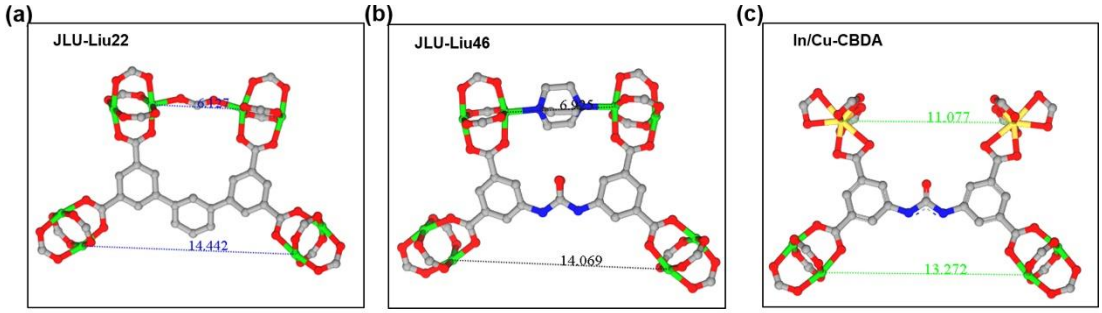

Figure S3. The center distance of the terminal benzenes of (a) **JLU-Liu22**, (b) **JLU-Liu46** and (c) **In/Cu-CBDA**.

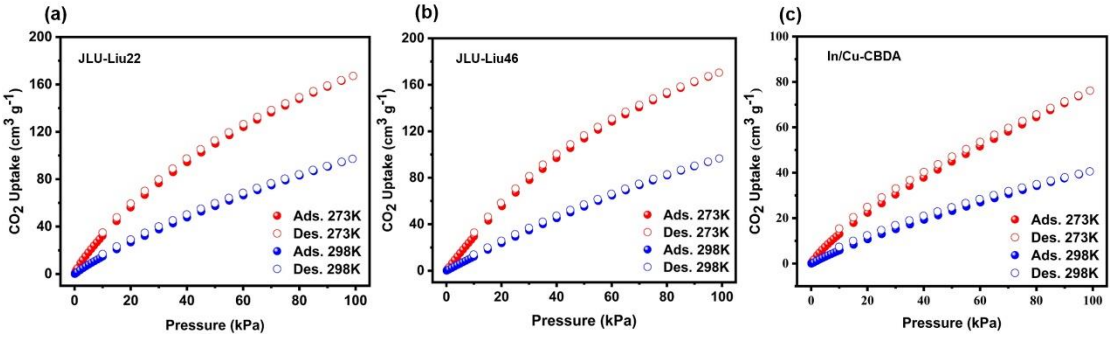

Figure S4. CO_2 adsorption and desorption isotherms of (a) **JLU-Liu46**, (b) **JLU-Liu22** and (c) **In/Cu-CBDA** at different temperatures.

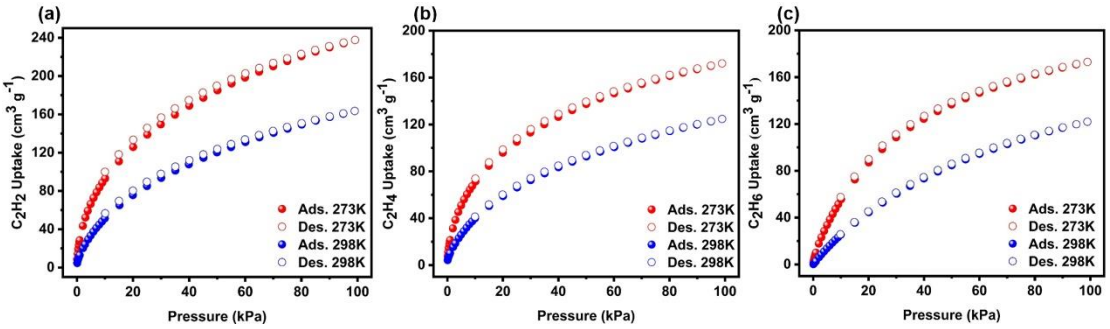

Figure S5. The adsorption and desorption isotherms of (a) C_2H_2, (b) C_2H_4 and (c) C_2H_6 for **JLU-Liu22** at different temperatures.

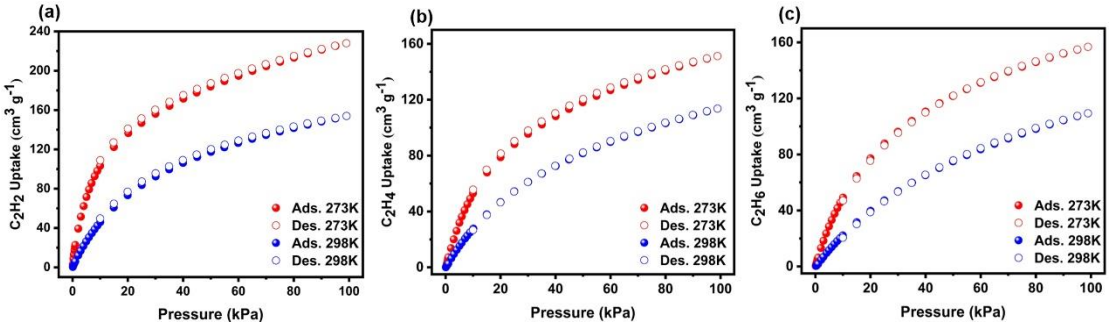

Figure S6. The adsorption and desorption isotherms of (a) C_2H_2, (b) C_2H_4 and (c) C_2H_6 for **JLU-Liu46** at different temperatures.

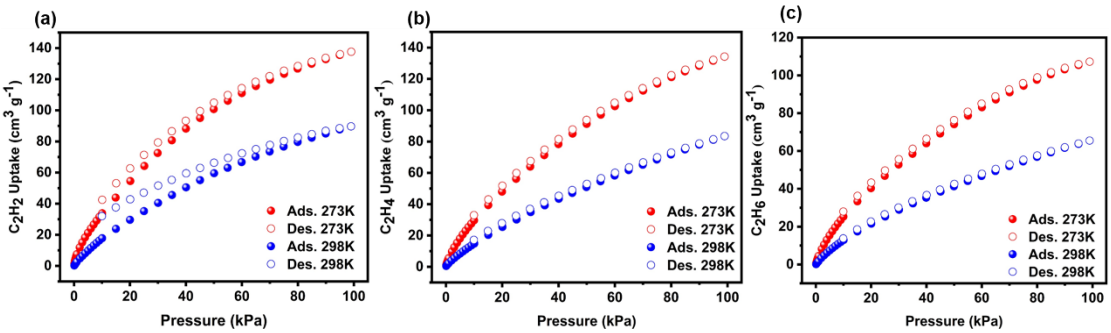

Figure S7. The adsorption and desorption isotherms of (a) C_2H_2, (b) C_2H_4 and (c) C_2H_6 for **In/Cu-CBDA** at different temperatures.

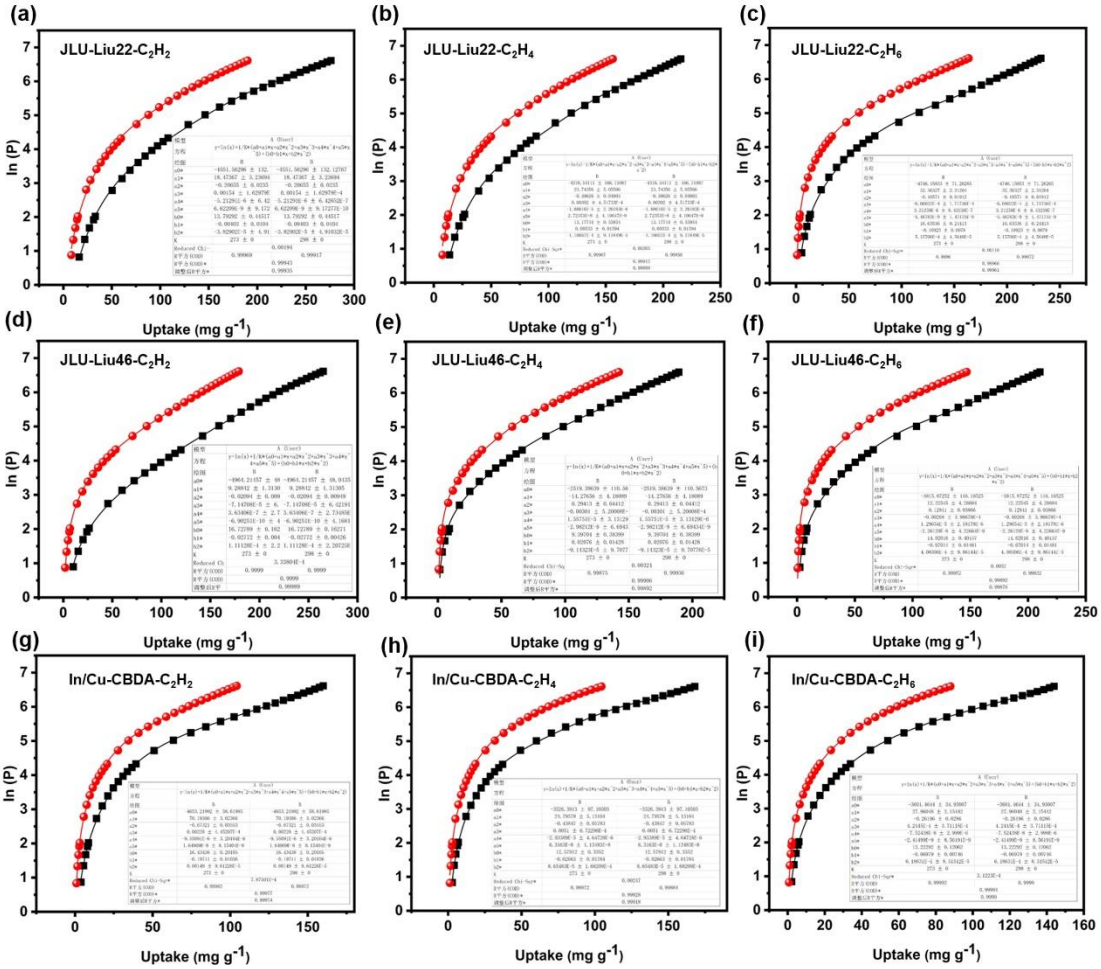

Figure S8. The fitting results of Q_{st} for (a) C_2H_2, (b) C_2H_4 and (c) C_2H_6 in **JLU-Liu22**, (d) C_2H_2, (e) C_2H_4 and (f) C_2H_6 in **JLU-Liu46**, (g) C_2H_2, (h) C_2H_4 and (i) C_2H_6 in **In/Cu-CBDA** by using adsorption isotherms at 298 K.

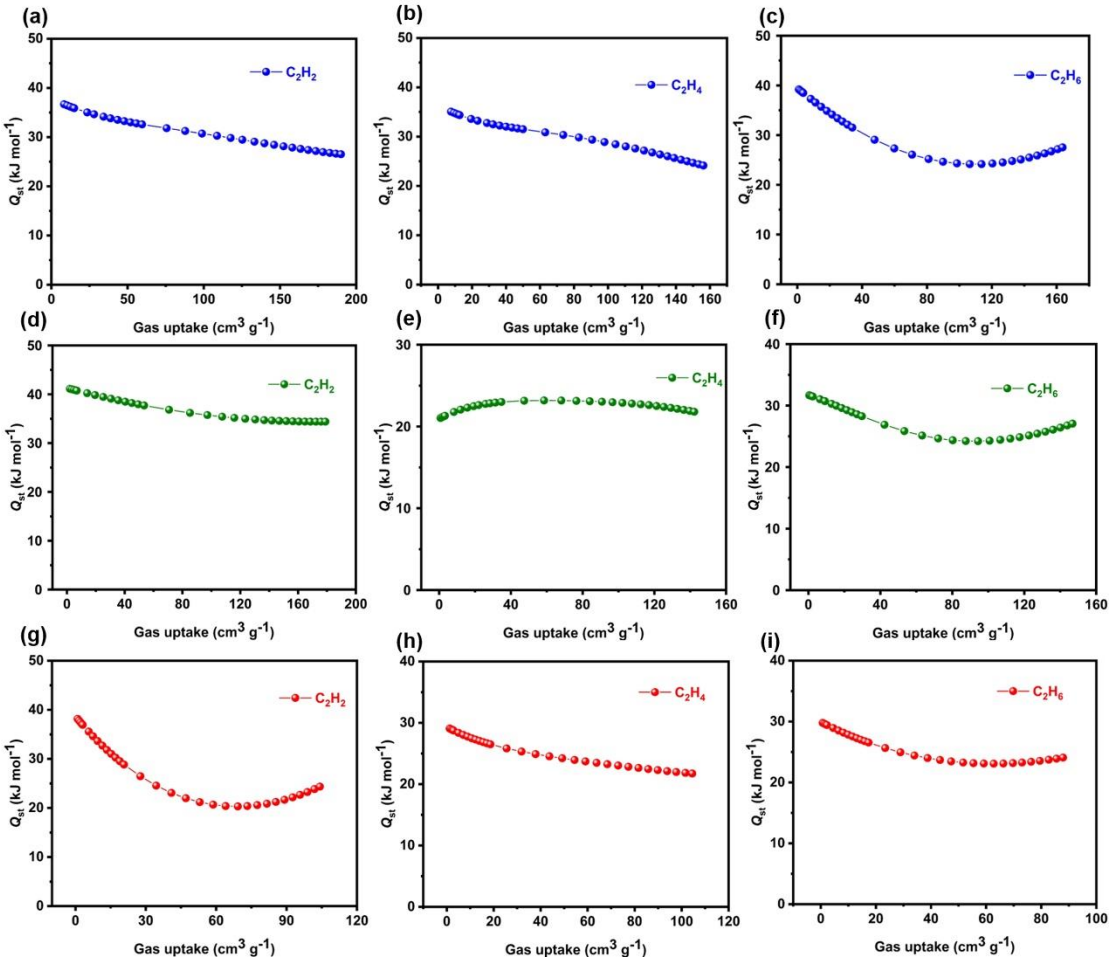

Figure S9. Q_{st} of C_2H_2, C_2H_4 and C_2H_6 for (a-c) **JLU-Liu22**, (d-f) **JLU-Liu46** and (g-i) **In/Cu-CBDA**, respectively.

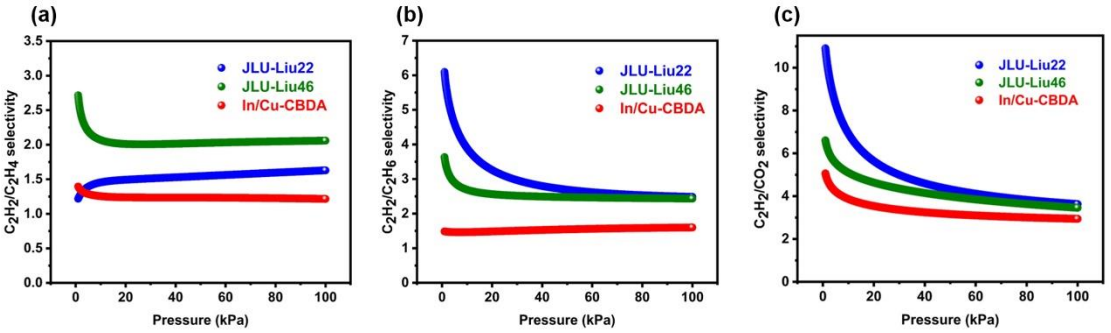

Figure S10. (a) C_2H_2/C_2H_4 (50/50), (b) C_2H_2/C_2H_6 (50/50) and (c) C_2H_2/CO_2 (50/50) adsorption selectivity are predicted by IAST at 298 K and 1 atm for compounds.

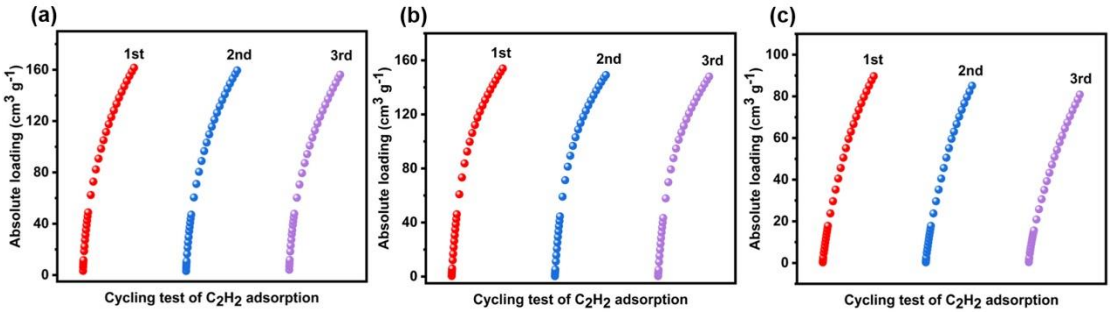

Figure S11. Repetitive C_2H_2 adsorption measurements of (a) **JLU-Liu22**, (b) **JLU-Liu46** and (c) **In/Cu-CBDA** at 298 K.

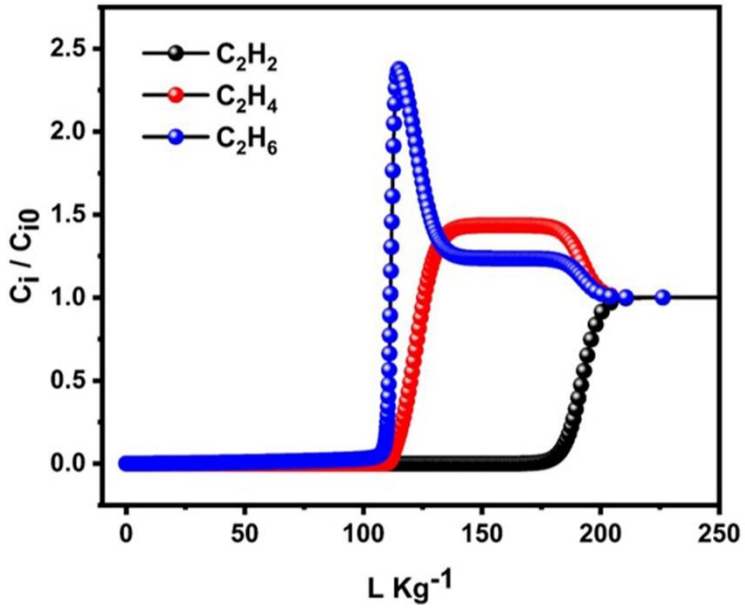

Figure S12. Simulations of transient breakthrough characteristics curves of **JLU-Liu46** for equimolar two-component $C_2H_2/C_2H_4/ C_2H_6$ mixtures at 100 kPa and 298 K

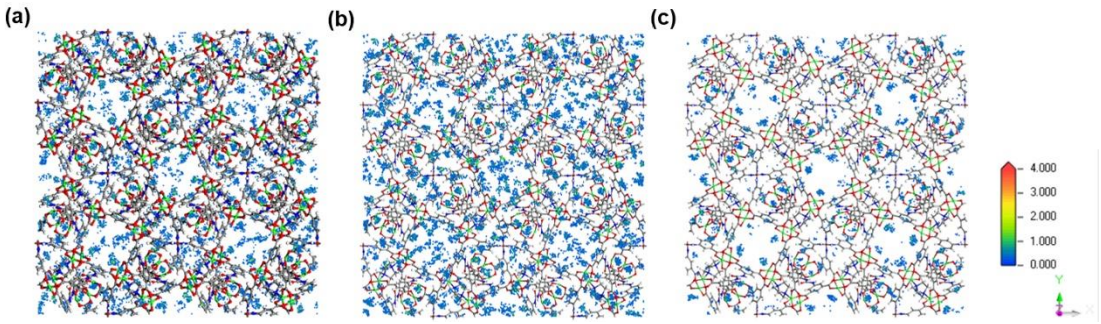

Figure S13. Density distribution of (a) C_2H_2, (b) C_2H_4 and (c) C_2H_6 molecules center-of-mass of **JLU-Liu46** at 298 K and 1 bar simulated by GCMC.

S2. Supporting Tables

Table S1. Physicochemical characteristics of different gasses relevant to their separation.

Molecules	**C_2H_2**	**C_2H_4**	**C_2H_6**
Dimensions (Å^3)	3.32×3.34×5.70	3.28×4.18×4.84	4.08×3.81×4.82
Kinetic diameter (Å)	3.3	4.2	4.4
Quadrupole moment ($\times10^{26}$ esu cm^2)	3.0	1.5	0.65
Polarisability (Å^3)	3.33-3.93	4.25	4.48
Boiling point (K)	189.4	169.5	184.6

Table S2. Summary of gas adsorption data for C_2H_2 separation materials at 298K and 1 bar.

Materials	**C_2H_2 Uptake (cm^3 g^{-1})**	**C_2H_2 Q_{st} (kJ mol^{-1})**	**Ref**
JLULiu-22	163.5	36.67	**This work**
JLULiu-46	153.9	41.11	**This work**
UPC-200(Fe)-F-BIM	139.7	20.5	[8]
PCP-33	121.8	27	[9]
MUF-15	109	24.5	[10]
JNU-2	103	15.8	[11]
NUM-12a	99.1	38.1	[12]
In/Cu-CBDA	89.7	38.2	**This work**
SIFSIX-3-Ni	74	36.7	[13]
UTSA-300a	68.9	57.6	[14]
JNU-1	60	13	[15]
BSF-1	52.6	31	[16]

Table S3. The refined parameters for the Dual-site Langmuir-Freundlich equations fit for the pure isotherms of C_2H_2, C_2H_4, C_2H_6 and CO_2 for **JLU-Liu22** at 298 K.

Adsorbate	**q_{m1} [mmol g^{-1}]**	**b_1 [kPa^{-1}]**	**n_1**	**q_{m2} [mmol g^{-1}]**	**b_2 [kPa^{-1}]**	**n_2**	**R^2**
C_2H_2	10.61993	0.0125	1	1	0.7435	0.9828	0.9996
C_2H_4	0.80603	0.7788	1	7.93224	0.0147	1	0.9996
C_2H_6	0.3035	0.1200	1.2596	9.35462	0.0095	1.0541	1
CO_2	1	0.0587	0.9914	11.6487	0.0015	1.2324	1

Table S4. The refined parameters for the Dual-site Langmuir-Freundlich equations fit for the pure isotherms of C_2H_2, C_2H_4, C_2H_6 and CO_2 for **JLU-Liu46** at 298 K.

Adsorbate	q_{m1} [mmol g^{-1}]	b_1 [kPa^{-1}]	n_1	q_{m2} [mmol g^{-1}]	b_2 [kPa^{-1}]	n_2	R^2
C_2H_2	9.59215	0.0315	0.9141	1	0.0038	1	0.9999
C_2H_4	2.36693	0.0355	1.1303	8.0345	0.006	1	0.9999
C_2H_6	0.95615	0.0277	1.2884	9.34812	0.0075	1	0.9999
CO_2	17.03436	0.00302	1.02426	0.00229	1	1	1

Table S5. The refined parameters for the Dual-site Langmuir-Freundlich equations fit for the pure isotherms of C_2H_2, C_2H_4, C_2H_6 and CO_2 for **In/Cu-CBDA** at 298 K.

Adsorbate	q_{m1} [mmol g^{-1}]	b_1 [kPa^{-1}]	n_1	q_{m2} [mmol g^{-1}]	b_2 [kPa^{-1}]	n_2	R^2
C_2H_2	5.76379	0.0023	1.3518	1	0.1060	0.9461	1
C_2H_4	1	0.0769	1	8.59628	0.0015	1.2603	0.9999
C_2H_6	1	0.0672	0.9520	7.72961	0.0018	1.1606	1
CO_2	0.30548	0.04109	1.13753	10.07197	0.00116	1.09449	1

References

(1) Wang, D.; Liu, B.; Yao, S.; Wang, T.; Li, G.; Huo, Q.; Liu, Y. A Polyhedral Metal-Organic Framework Based on the Supermolecular Building Block Strategy Exhibiting High Performance for Carbon Dioxide Capture and Separation of Light Hydrocarbons. *Chem. Commun.* **2015**, *51* (83), 15287-15289.

(2) Liu, B.; Yao, S.; Liu, X.; Li, X.; Krishna, R.; Li, G.; Huo, Q.; Liu, Y. Two Analogous Polyhedron-Based Mofs with High Density of Lewis Basic Sites and Open Metal Sites: Significant CO_2 Capture and Gas Selectivity Performance. *ACS Appl. Mater. Interfaces* **2017**, *9* (38), 32820-32828.

(3) Wang, D.; Zhang, Y.; Gao, J.; Ge, G.; Li, C. A Polyhedron-Based Heterometallic Mof Constructed by Hsab Theory and Sbb Strategy: Synthesis, Structure, and Adsorption Properties. *Cryst. Growth Des.* **2019**, *19* (8), 4571-4578.

(4) Krishna, R. The Maxwell–Stefan Description of Mixture Diffusion in Nanoporous Crystalline Materials. *Microporous Mesoporous Mater.* **2014**, *185*, 30-50.

(5) Krishna, R. Methodologies for Evaluation of Metal–Organic Frameworks in Separation Applications. *RSC Advances* **2015**, *5* (64), 52269-52295,

(6) Krishna, R. Screening Metal–Organic Frameworks for Mixture Separations in Fixed-Bed Adsorbers Using a Combined Selectivity/Capacity Metric. *RSC Advances* **2017**, *7* (57), 35724-35737.

(7) Metropolis, N.; Rosenbluth, A. W.; Rosenbluth, M. N.; Teller, A. H.; Teller, E. Equation of State Calculations by Fast Computing Machines. *J. Chem. Phys.* **1953**, *21* (6), 1087-1092.

(8) Fan, W.; Yuan, S.; Wang, W.; Feng, L.; Liu, X.; Zhang, X.; Wang, X.; Kang, Z.; Dai, F.; Yuan, D.; Sun, D.; Zhou, H. C. Optimizing Multivariate Metal-Organic Frameworks for Efficient C_2H_2/CO_2 Separation. *J. Am. Chem. Soc.* **2020**, *142* (19), 8728-8737.

(9) Duan, J.; Jin, W.; Krishna, R. Natural Gas Purification Using a Porous Coordination Polymer with Water and Chemical Stability. *Inorg. Chem.* **2015**, *54* (9), 4279-4284.

(10) Qazvini, O. T.; Macreadie, L. K.; Telfer, S. G. Effect of Ligand Functionalization

on the Separation of Small Hydrocarbons and CO_2 by a Series of Muf-15 Analogues. *Chem. Mater.* **2020**, *32* (15), 6744-6752.

(11) Xie, X.-J.; Zeng, H.; Xie, M.; Chen, W.; Hua, G.-F.; Lu, W.; Li, D. A Metal-Organic Framework for C_2H_2/CO_2 Separation under Highly Humid Conditions: Balanced Hydrophilicity/Hydrophobicity. *Chem. Eng. J.* **2022**, *427*, 132033.

(12) Zhang, Q.; Yang, S. Q.; Zhou, L.; Yu, L.; Li, Z. F.; Zhai, Y. J.; Hu, T. L. Pore-Space Partition through an Embedding Metal-Carboxylate Chain-Induced Topology Upgrade Strategy for the Separation of Acetylene/Ethylene. *Inorg. Chem.* **2021**, *60* (24), 19328-19335.

(13) Zhang, Z.; Ding, Q.; Cui, J.; Cui, X.; Xing, H. Fine-Tuning Pore Dimension in Hybrid Ultramicroporous Materials Boosting Simultaneous Trapping of Trace Alkynes from Alkenes. *Small* **2020**, *16* (49), e2005360.

(14) Lin, R. B.; Li, L.; Wu, H.; Arman, H.; Li, B.; Lin, R. G.; Zhou, W.; Chen, B. Optimized Separation of Acetylene from Carbon Dioxide and Ethylene in a Microporous Material. *J. Am. Chem. Soc.* **2017**, *139* (23), 8022-8028.

(15) Zeng, H.; Xie, M.; Huang, Y. L.; Zhao, Y.; Xie, X. J.; Bai, J. P.; Wan, M. Y.; Krishna, R.; Lu, W.; Li, D. Induced Fit of C_2h_2 in a Flexible Mof through Cooperative Action of Open Metal Sites. *Angew. Chem., Int. Ed. Engl.* **2019**, *58* (25), 8515-8519.

(16) Zhang, Y.; Yang, L.; Wang, L.; Duttwyler, S.; Xing, H. A Microporous Metal-Organic Framework Supramolecularly Assembled from a Cu(II) Dodecaborate Cluster Complex for Selective Gas Separation. *Angew. Chem., Int. Ed. Engl.* **2019**, *58* (24), 8145-8150.